Mercury Binding to Nucleic Acids. Crystal and Molecular Structures of 2:1 Complexes of Uracil–Mercuric Chloride and Dihydrouracil–Mercuric Chloride*

J. A. Carrabine† and M. Sundaralingam‡

ABSTRACT: The structures of the 2:1 complexes of uracil–mercuric chloride, $(C_4H_4N_2O_2)_2HgCl_2$, and dihydrouracil (a minor base of tRNA) mercuric chloride, $(C_4H_6N_2O_2)_2HgCl_2$, have been determined using three-dimensional X-ray data measured on a diffractometer. Crystals of uracil–mercuric chloride are triclinic space group $P\bar{1}$ with unit cell constants $a = 6.898 \pm 0.004$ Å, $b = 3.951 \pm 0.001$ Å, $c = 11.835 \pm 0.007$ Å, $\alpha = 88.57 \pm 0.03°$, $\beta = 101.44 \pm 0.01°$, and $\gamma = 87.03 \pm 0.03°$, while crystals of dihydrouracil–mercuric chloride are monoclinic, space group $P2_1/a$ with unit cell constants $a = 7.600 \pm 0.004$ Å, $b = 7.128 \pm 0.004$ Å, $c = 12.457 \pm 0.005$ Å, and $\beta = 94.84 \pm 0.02°$. The calculated and observed densities are, respectively, 2.608, 2.608 g cm^{-3} for uracil–mercuric chloride and 2.47 (assuming $Z = 2$), and 2.42 g cm^{-3} in dihydrouracil–mercuric chloride. The structures were determined by the heavy-atom technique and refined by full-matrix least squares to R values of 0.09 and 0.11 for the uracil and dihydrouracil complexes, respectively. The mercury atoms are held by chlorine bridges with the octahedral coordination completed by the keto oxygens, O(4), of inversion-related bases.

The bonding here is quite different from that previously proposed for mercury interaction with DNA. The uracils in the complex are hydrogen bonded to one another through pairs of N(3)–H · · · O(2) and N(1)–H · · · O(2) hydrogen bonds forming infinite zigzag chains. The dihydrouracils are also hydrogen bonded by the same pair of hydrogen bonds; the only difference being that here the bases are not center related. The mercury atoms are markedly displaced from the base planes.

The interaction of metal ions with nucleic acids and their constituents has received considerable attention in recent years (Eichhorn and Shin, 1968; Yamane and Davidson, 1961). The importance of these phenomena lies in the possible biological role of these metals in nucleic acid processes as well as the use of model nucleic acid–metal compounds in the understanding of the complex structures of the nucleic acids themselves.

In general, metal ion interactions with double-stranded DNA can be divided into two classes. Most monovalent ions and some divalent cations (*e.g.*, Na^+, Mn^{2+}, and Co^{2+}) are thought to bind to the negatively charged sugar–phosphate backbone, thus contributing to the stability of the ordered double helix. The second class of ions (*e.g.*, Cd^{2+}, Cu^{2+}, and Pb^{2+}) bind preferentially to the heterocyclic bases, disrupting the hydrogen bonding, and hastening the denaturation of the ordered structure (Eichhorn and Shin, 1968). We are particularly interested in the latter type of behavior since it represents a departure from the normal biological processes. The understanding of these phenomena has been hampered by a lack of knowledge concerning the metal binding sites on the bases. We are engaged in a continuing study of selected metal ions with the nucleic acid components, utilizing X-ray crystallographic techniques.

Another base binding metal, Hg^{2+}, is unique in its ability to form complexes with native DNA at room temperature (Yamane and Davidson, 1961). Other metals, such as Cu^{2+}, require thermal assistance for base binding, *i.e.*, apparently, the helix must be partially unwound exposing the base sites for attack by the Cu^{2+} ion. Extensive studies have been carried out on mercury–DNA interactions (Yamane and Davidson, 1961; Gruenweldel and Davidson, 1966, 1967; Eichhorn and Clark, 1963; Simpson, 1964; Matsuda and Takeuchi, 1967) with the general conclusion that mercury is bound to the nitrogen atoms of the heterocyclic bases. Moreover, Davidson and coworkers (Nandi *et al.*, 1965) report that the binding is selective, AT-rich DNAs binding more strongly than GC-rich DNAs. In a suggested structure they show mercury binding to N(3) of thymidine, a site normally protonated, and involved in hydrogen bonding to adenosine in the Watson–Crick model. Their observation of proton release upon complex formation is consistent with the proposed model. However, the required interaction of mercury with well-protected sites within the ordered helix does little to explain the ease with which the complex forms with native DNA. Copper is known to bind to a similarly protected site, N(3) of cytosine (Carrabine and Sundaralingam, 1968; J. A. Carrabine and M. Sundaralingam, in preparation), but in this case, partial thermal denaturation is required before complex formation occurs.

We are presently investigating mercury complexes with the nucleic acid constituents. The knowledge gained in this work would be helpful in the structural investigation of single crystals of tRNA by the heavy-atom and isomorphous methods of X-ray crystallography. Here we present the crystal structures of 1:2 mercuric chloride complexes with both uracil and dihydrouracil. These should be analogous to

---

* From the Department of Chemistry, Case Western Reserve University, Cleveland, Ohio 44106. *Received May 21, 1970.* This paper is part XVI in a series of papers on the Stereochemistry of Nucleic Acids and Their Constituents. For part XV, see Lin and Sundaralingam (1971). This work was supported by a research grant (GM 14828) from the National Institute of General Medical Sciences of the U. S. Public Health Service. Communicated at the VIII International Union of Crystallography Congress, Buffalo, N. Y.

† Present address: Department of Chemistry, John Carroll University, Cleveland, Ohio.

‡ Present address: Department of Biochemistry, University of Wisconsin, Madison, Wis. 53706; to whom correspondence should be directed.

the thymine–mercury complex noted above (Nandi *et al.*, 1965).

Experimental Section

Crystal Structure of Uracil–Mercuric Chloride Complex. Colorless, translucent crystals of $(C_4H_4N_2O_2)_2HgCl_2$ were prepared by heating a solution of 9.72 mM of uracil in 2.4 ml of 0.02 M $HgCl_2$ solution (4.86 mM) for about 5 min and allowing the solution to evaporate at room temperature. The initial pH of the $HgCl_2$ solution was 4.2. The crystals were generally prismatic and elongated along the *b* axis. Preliminary oscillation and Weissenberg photographs of one of the crystals of dimensions 0.2 × 0.2 × 0.4 mm showed that it was triclinic and gave the values for a^*, c^*, and β^*. Precession photographs about both the *a* and *c* axes were then used to obtain b^*, α^*, and γ^*. Crystal data, including the unit cell constants obtained by using our diffractometer, are given in Table I.

TABLE I: Crystal Data for Uracil.

	Mercury(II) Chloride
Formula	$Hg(C_4N_2H_4O_2)_2Cl_2$
System	Triclinic
Systematic absences	None
Space group	P1, by structure analysis
a (Å)	6.898 ± 0.004
b (Å)	3.951 ± 0.001
c (Å)	11.835 ± 0.007
α	88.57 ± 0.03
β	101.44 ± 0.07
γ	87.03 ± 0.03
λ(Cu Kα) (Å)	1.5418
Volume (Å^3)	315.5
Molecular weight	495.67
Z	$2(C_4H_4N_2O_2\cdot Hg_{0.5}Cl)$
D_{calcd} (g cm^{-3})	2.608
D_{obsd} (g cm^{-3})	2.608, flotation in bromoform–carbon tetrachloride

Three-dimensional intensity data were collected on a crystal mounted about the *b* axis, using the Picker four-circle automatic diffractometer, nickel-filtered Cu Kα radiation, and a 2θ scan mode at a scan speed of 2°/min. Reflections were considered as unobservable if $I < 1 \cdot 4\sigma(I)$, where $\sigma(I) = [I + B + [k_i \cdot (I - B)]^2]^{1/2}$, where I = total scanned intensity, B = total background intensity, k_i = a constant related to instrumental stability (=0.05). On this basis, all but 8 of the 1094 unique reflections measured, were considered to be observable. The data were corrected for Lorentz and polarization factors and each reflection was assigned a weight.

$$1/\sqrt{w} = \sigma(F) = \frac{k}{2\sqrt{Lp}}\left(\frac{I + B + [k_i(I - B)]^2}{I - B}\right)^{1/2}$$

where k = scale constant, and $1/Lp$ is the Lorentz polarization factor. No correction for absorption was made.

The calculated and observed densities (Table I) clearly indicate the presence of only one mercury atom per unit cell. Accordingly, the mercury atom must lie at the origin. In these circumstances, the Patterson function will show Hg–Hg interactions only at the origin of the Patterson map. Furthermore, the Hg–light atom interactions will appear as prominent peaks whose Patterson coordinates correspond to their unit cell coordinates. An unsharpened, three-dimensional Patterson map was prepared with sections calculated along the *b* axis. Since the latter has a length close to the intermolecular stacking distance for bases, this direction was expected to provide a view roughly normal to the uracil ring. Analysis of the Patterson map confirmed this expectation and both the uracil and chlorine atoms were readily located. At this point the orientation of the uracil ring could not be unambiguously assigned, although preliminary considerations of hydrogen-bonding schemes suggested the labeling of the uracil atoms which turned out to be correct.

An initial structure factor calculation based on the model gave a value of 0.24 for the conventional R factor $R = \Sigma\,||F_o| - |F_c||/\Sigma|F_o|$. Two cycles of isotropic full-matrix least-squares refinement, varying all of the parameters except the position of mercury, gave an R factor of 0.14. Several additional cycles of anisotropic refinement gave the final R factor of 0.093. The scattering factors of Cromer and Waber (1965) were used and the real part of the anomolous dispersion correction was applied to mercury and chlorine during the final refinement. The relatively high value of R is undoubtedly associated with the very high absorption due to mercury and chlorine. As noted earlier, absorption corrections were not made. The final positional and thermal parameters are given in Table II.

Crystal Structure of Dihydrouracil–Mercuric Chloride Complex. Crystals of $(C_4N_2H_6O_2)_2H_gCl_2$ were prepared by dissolving 10.4 mg of dihydrouracil (0.090 mM) in 2.25 ml of 0.02 M $HgCl_2$ (0.045 mM) and allowing the solution to evaporate after a brief gentle heating. Relatively large, translucent rods were obtained, which cleaved very easily. Examination of a large number of crystals revealed only a few suitable for single crystal analysis. Oscillation and Weissenberg photographs showed the crystal to be monoclinic, space group $P2_1/a$, and elongated in the *a* direction. Pertinent crystal data together with unit cell constants obtained by the use of the diffractometer are given in Table III.

A total of 1152 unique reflections was measured on the diffractometer; of these 260 were considered as unobservable by the criterion described earlier. Preliminary work had shown that the crystals were unstable under prolonged X-radiation, hence the crystal was mounted in a Lindemenn glass capillary. Despite this precaution, the first crystal deteriorated badly during the first half of the data collection, the loss in the standard intensity being approximately 20%, and a second crystal had to be used to complete the data collection. The data were reduced and weighted in the same manner as before.

From the calculated and observed densities (Table III) it was clear that mercury must lie at special positions. Examination of the Weissenberg photographs showed alternately weak and strong festoons when $h + k$ was odd and even, respectively. This corresponds to a pseudo C centering. Since mercury dominates the scattering, it was therefore assumed that the mercury atom occupies the special positions (0, 0, 0) and ($^1/_2$, $^1/_2$, 0). An unsharpened Patterson synthesis confirmed this assumption and also revealed the chlorine positions. An initial structure factor calculation, using the mercury and chlorine positions gave an R factor of 0.33. A difference Fourier using $F_{\mathrm{obsd}} - F_{\mathrm{Hg,Cl}}$ as coefficients clearly revealed the dihydrouracil ring.

Two cycles of isotropic refinement using all of the non-

TABLE II: Positional and Thermal[a] Parameters and Their Estimated Standard Deviations × 10^4 in Parentheses for Uracil–Mercury(II) Chloride.

Atom	x	y	z	β_{11}	β_{22}	β_{33}	β_{12}	β_{13}	β_{23}
Hg	0	0	0	117 (3)	536 (11)	46 (1)	−24 (4)	19 (1)	−48 (2)
Cl	2637 (9)	6054 (15)	0362 (5)	167 (12)	582 (38)	71 (5)	−46 (17)	13 (6)	−52 (11)
N(1)	5456 (28)	2404 (57)	3754 (16)	124 (39)	798 (159)	4 (13)	−34 (63)	24 (18)	−41 (36)
N(3)	8782 (30)	2509 (54)	3720 (17)	160 (43)	657 (143)	47 (14)	−79 (63)	18 (19)	−32 (35)
O(2)	7533 (24)	5067 (55)	5120 (16)	131 (37)	1076 (170)	68 (14)	−85 (63)	35 (18)	−133 (39)
O(4)	10125 (26)	312 (62)	2297 (16)	148 (37)	1260 (203)	61 (13)	−92 (69)	41 (18)	−105 (42)
C(2)	7270 (31)	3425 (65)	4231 (19)	105 (43)	738 (174)	46 (16)	−53 (69)	22 (21)	−46 (42)
C(4)	8605 (33)	797 (73)	2715 (19)	121 (47)	969 (211)	37 (15)	−18 (78)	28 (21)	−40 (44)
C(5)	6633 (38)	−206 (73)	2242 (21)	193 (58)	856 (205)	49 (17)	−141 (89)	35 (25)	−73 (48)
C(6)	5164 (35)	643 (59)	2745 (20)	146 (49)	796 (187)	47 (16)	59 (77)	35 (23)	−37 (44)

[a] β_{ij}'s are defined by the expression: $T = \exp[-(\beta_{11}h^2 + \beta_{22}k^2 + \beta_{33}l^2 + 2\beta_{12}hk + 2\beta_{13}hl + 2\beta_{23}kl)]$.

hydrogen atoms gave an R factor of 0.20. A cycle of anisotropic refinement dropped the R factor to 0.12. Possible hydrogen positions were obtained from a difference Fourier map at this point. A final cycle of anisotropic refinement varying all positional parameters except those of mercury, and all thermal parameters except those of hydrogen, gave the present R factor of 0.11. As in the case of the uracil complex, the relatively high value of R is largely due to absorption. In addition, crystal deterioration during data collection could have introduced errors in the data. The final positional and thermal parameters are given in Table IV.

Description of the Structures. URACIL–MERCURIC CHLORIDE. The molecular structure of the uracil–mercuric chloride complex, as viewed along the b and a axes, respectively, is shown in Figures 1 and 2, respectively. The mercury atom is bonded to the O(4) atoms of inversion-related uracil rings. The bases in turn are hydrogen bonded to one another through pairs of N(3)–H· · · ·O(2) and N(1)–H· · · ·O(2)–hydrogen bonds forming a zig-zag chain. The mercury-bound-O(4) atom does not participate in hydrogen bonding. The hydrogen bonding here is very similar to that found in dihydrouracil (Rohrer and Sundaralingam, 1970). In the latter, the O(4) atom is again not involved in hydrogen bonding, and two zigzag chains are held together by weak van der Waals forces. In contrast, uracil itself (Stewart and Jensen, 1967) involves center-related N(3)–H · · · · O(4) pairs and a single N(1)–H · · · · O(4) bond. The O(2) atom does not participate in hydrogen bonding although it is involved in close intermolecular contacts with C–H ring atoms. Evidently the O(4) is more susceptible to electrophilic attack since mercury attaches to it rather than to O(2). In this respect it is found that protonation of 1-methyluracil also occurs at O(4) (Sobell and Tomita, 1964). In the related complex described in the next section, O(4) is again the preferred site. The hydrogen bonding in the present structure differs from that of the conventional Watson–Crick scheme in that the uracil is bonded to adenine through its O(4) and N(3)–H sites and O(2) is not utilized.

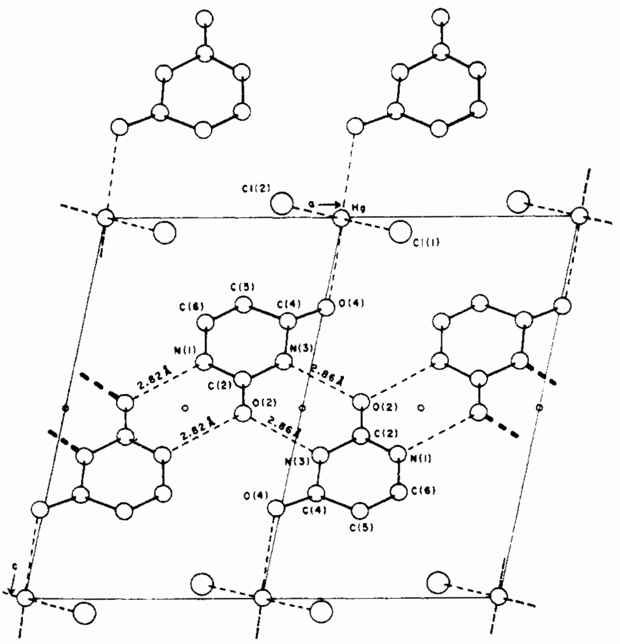

FIGURE 1: The intermolecular hydrogen bonding and mercury coordination in uracil–mercuric chloride, viewed along the b axis.

TABLE III: Crystal Data for Dihydrouracil–Mercury(II) Chloride.

Formula	$(C_4N_2H_6O_2)_2HgCl_2$
Crystal system	Monoclinic
Systematic absences	$h0l$, $h = 2n + 1$ $0k0$, $k = 2n + 1$
Space group	$P2_1/a$
a (Å)	7.600 ± 0.004
b (Å)	7.128 ± 0.004
c (Å)	12.457 ± 0.005
β (deg)	94.842 ± 0.016
λ(Cu Kα) (Å)	1.5418
Volume (Å^3)	672.4
Molecular weight	499.8
Z	2
D_{calcd} (g cm^{-3})	2.468
D_{obsd} (g cm^{-3})	2.422, by flotation in carbon tetrachloride–bromoform solution

TABLE IV: Positional and Thermal Parameters[a] and Their Estimated Standard Deviations × 10^4 in Parentheses for Dihydrouracil–Mercury(II) Chloride.

Atom									
Hg	0 (0.0)	0 (0.0)	0 (0.0)	207 (4)	70 (4)	48 (1)	−14 (3)	−11 (2)	−7 (2)
Cl	2207 (13)	2097 (9)	0461 (7)	274 (19)	77 (10)	63 (6)	−8 (12)	−08 (9)	2 (7)
O(2)	7635 (38)	9237 (24)	5113 (18)	357 (66)	63 (30)	39 (16)	−12 (37)	−33 (26)	−14 (18)
O(4)	5212 (40)	5949 (30)	2257 (20)	375 (78)	89 (42)	62 (19)	9 (44)	−21 (31)	−26 (22)
N(1)	6238 (40)	10841 (33)	3702 (23)	245 (65)	45 (36)	57 (20)	−14 (38)	−19 (29)	−6 (21)
N(3)	6275 (39)	7633 (28)	3691 (20)	316 (28)	40 (36)	41 (19)	−23 (37)	−16 (28)	−12 (19)
C(2)	6760 (48)	9326 (35)	4237 (23)	268 (79)	46 (41)	34 (20)	−28 (42)	3 (33)	−7 (21)
C(4)	5659 (43)	7484 (35)	2648 (25)	240 (70)	42 (44)	44 (24)	−28 (41)	−3 (33)	−9 (23)
C(5)	5436 (51)	9256 (42)	2048 (30)	293 (81)	73 (51)	51 (25)	119 (51)	−38 (37)	−17 (29)
C(6)	5022 (54)	10885 (45)	2771 (27)	362 (96)	109 (58)	36 (24)	48 (57)	−49 (38)	−11 (30)
H(1)[b]	640 (49)	1169 (44)	404 (28)						
H(3)	699 (45)	103 (41)	418 (25)						
H(5)	498 (53)	1001 (41)	119 (33)						
H(5′)	437 (43)	882 (43)	137 (25)						
H(6)	530 (51)	1186 (49)	227 (28)						
H(6′)	510 (58)	931 (48)	192 (31)						

[a] β_{ij}'s are defined by the expression: $T = \exp[-(\beta_{11}h + \beta_{22}k^2 + \beta_{33}l^2 + 2\beta_{12}hk + 2\beta_{13}hl + 2\beta_{23}kl)]$. [b] The hydrogen atoms were given the anisotropic thermal parameters of the atoms to which they were attached.

Bond lengths and bond angles for the mercury–uracil complex and for uracil itself are compared in Table V. The relatively high standard deviations preclude any detailed comparison except to note the general agreement between the two structures. The C(4)–O(4) bond distance of 1.245 Å in uracil is typical of keto groups involved in hydrogen bonding with other bases (the normal C=O bond length being 1.20–1.21 Å; see C(2)–O(2) of uracil, Table V). For the complex, O(4) is bonded directly to mercury. It seems that metal binding has essentially the same effect on bond lengths as does hydrogen bonding. Similarly, protonation of O(4), occurring in 1-methyluracil hydrobromide (Sobell and Tomita, 1964), increases the C(4)–O(4) bond length to 1.28 Å. The O(2) atom of the complex is involved in hydrogen bonding, and it is seen that the corresponding C(2)–O(2) bond length is also lengthened.

The planes of the uracil bases lie parallel to one another and are roughly parallel with the 01$\bar{1}$ crystal planes (Figure 2). A number of intermolecular contacts are also shown in Figure 2. The interplanar distance is 3.31 Å. A view of the base

TABLE V: Comparison of Bond Lengths and Bond Angles for the Uracil Ring.

	Bond Lengths (Å)[b]	
	HgU_2Cl_2	Uracil[a]
N(1)–C(2)	1.35 (3)	1.371 (2)
C(2)–N(3)	1.34 (3)	1.376 (2)
N(3)–C(4)	1.37 (3)	1.371 (2)
C(4)–C(5)	1.44 (3)	1.430 (2)
C(5)–C(6)	1.31 (4)	1.340 (2)
C(6)–N(1)	1.38 (3)	1.358 (2)
C(2)–O(2)	1.24 (2)	1.215 (2)
C(4)–O(4)	1.25 (3)	1.245 (2)
	Bond Angles (deg)[c]	
N(1)–C(2)–N(3)	117 (2)	114.0 (1)
C(2)–N(3)–C(4)	125 (2)	126.7 (2)
N(3)–C(4)–C(5)	115 (2)	115.5 (1)
C(4)–C(5)–C(6)	120 (2)	118.9 (2)
C(5)–C(6)–N(1)	121 (2)	122.3 (2)
C(6)–N(1)–C(2)	121 (2)	122.7 (1)
N(1)–C(2)–O(2)	121 (2)	123.7 (2)
N(3)–C(2)–O(2)	121 (2)	122.3 (2)
N(3)–C(4)–O(4)	118 (2)	119.2 (2)
C(5)–C(4)–O(4)	127 (2)	125.3 (2)

[a] Stewart and Jensen (1967). [b] Estimated standard deviations in parentheses are in the last digit. [c] Estimated standard deviations in degrees in parentheses.

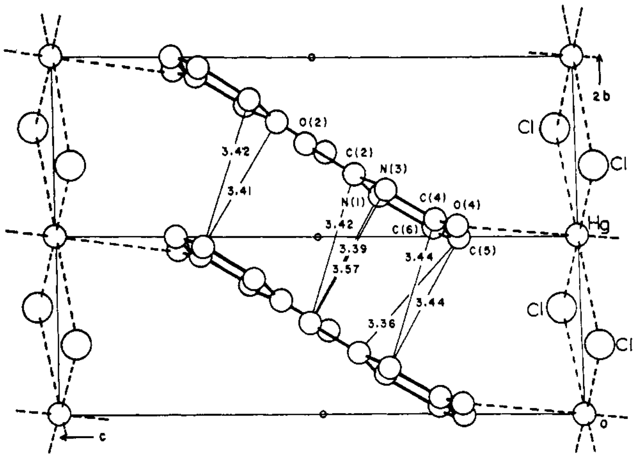

FIGURE 2: View along the *a* axis of uracil mercuric chloride showing the molecular packing, interbase distances, and the infinite Cl–Hg–Cl chain along the *b* axis.

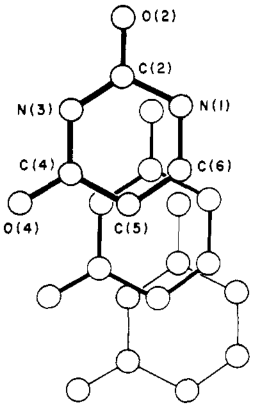

FIGURE 3: The mode of stacking of the uracil bases in uracil mercuric chloride viewed normal to the bases.

stacking is shown in Figure 3. The relatively small amount of base overlap is consistent with the trend for pyrimidine bases, in general, and with other uracil derivatives (Sundaralingam *et al.*, 1969; Bugg *et al.*, 1971).

The least-squares plane for the uracil ring atoms is given in Table VI. As seen, the ring is planar within one standard deviation. Mercury, however, is 1.5 Å above the plane. The O(4) atom is significantly out of plane in the direction of mercury to which it is bound. Since the same atom in uracil (Stewart and Jensen, 1967) is only slightly out of the plane of the base (0.017 Å) the distortion here is attributed in part to metal binding.

Dihydrouracil–Mercuric Chloride. The structure of the complex as viewed down the *a* axis is shown in Figure 4. As in the case of the previous complex, mercury is bound to O(4) atoms of inversion related rings, with its octahedral coordination completed by four chlorines. Again it is seen that mercury combines as $HgCl_2$ rather than Hg^{2+} ion. A notable difference in this structure is that the Hg–Cl network forms parallel sheets with each mercury atom being linked to four other mercury atoms through chlorine bridges. In the case of the uracil complex above, infinite Cl–Hg–Cl chains were observed.

TABLE VI: Deviations of the Atoms from the Least-Squares Plane in Uracil–Mercury(II) Chloride.[a]

Atom	Deviation (Å)
Hg	1.50
Cl	3.24
N(1)	−0.01
N(3)	−0.02
O(2)	0.03
O(4)	0.07
C(2)	0.02
C(4)	0.01
C(5)	−0.01
C(6)	0.01

[a] The equation for the least-squares plane is $lx + my + nz = d$ where l, m, and n are the direction cosines of the normal to the plane, and d is the distance of the plane from the origin in angstrom units; x, y, and z are coordinates in angstrom units; $l = -0.027$, $m = 0.839$, $n = -0.542$, and $d = -1.501$. [b] Atoms included in the calculation of the least-squares plane are shown in bold type.

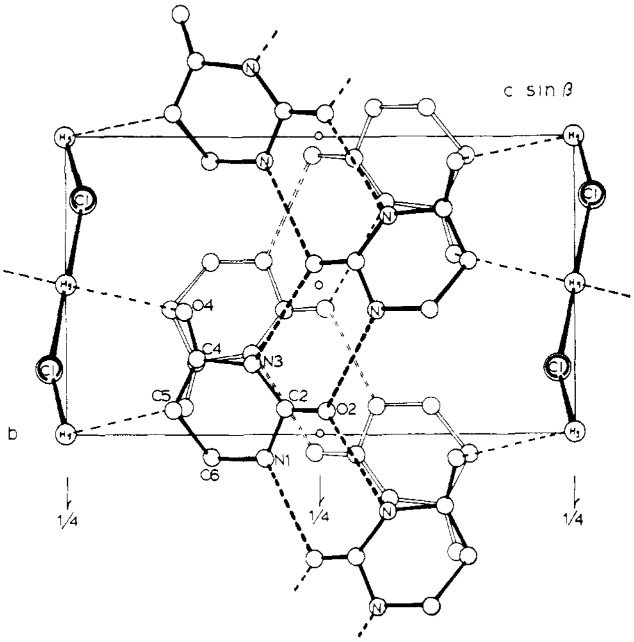

FIGURE 4: View along the *a* axis showing the molecular packing hydrogen bonding and mercury coordination in dihydrouracil mercuric chloride.

In addition to mercury binding, the bases are hydrogen bonded to one another in a zigzag fashion in a plane roughly diagonal to the plane containing the Hg and Cl atoms. In contrast to both the uracil–mercuric chloride complex and to dihydrouracil (Rohrer and Sundaralingam, 1970) itself, the hydrogen bonding involves N(3)–H · · · O(2) and N(1)–H · · · O(2) pairs (Figure 4) rather than the center-related bases.

The bond lengths and bond angles for the dihydrouracil portion of the complex are compared to those of dihydrouracil in Table VII. The values agree within the experimental errors.

Some least-squares planes are given in Table VIII, while torsional angles for the complex and for dihydrouracil are presented in Table IX. As expected, the saturation of the C(5)–C(6) bond results in a puckered (twist half-chair) conformation for the pyrimidine ring, essentially the same as that found in dihydrouracil (Rohrer and Sundaralingam, 1970) (Table IX). C(5) and C(6) are displaced by 0.2 and 0.4 Å on opposite sides from the four-atom plane (plane 2, Table VIII). Both the carbonyl oxygen atoms are also displaced significantly on opposite sides from the pyrimidine ring plane. The deviation of the Hg atom from the base plane is 0.607 Å.

The interplanar separation in this complex is 3.36 Å based on plane 2 in Table VIII. Again there is hardly any overlap of adjacent rings (Figure 4).

Mercury Coordination. A significant feature found in both structures is that mercury combines as $HgCl_2$ rather than as Hg^{2+}. The coordination of mercury in the structures is shown in Figures 2 and 4, and bond lengths and angles involved in the coordination sphere are given in Table X. While mercury characteristically forms two short, linear bonds, it generally coordinates to additional ligands to increase its coordination number. Hence, the distorted octahedral geometries observed here, possessing two short and four long bonds, are typical of mercury coordination (Grdenic, 1965). Both complexes

TABLE VII: Bond Lengths and Bond Angles for Dihydrouracil–Mercury(II) Chloride and Dihydrouracil.

Bond	Bond Lengths (Å)[a]	
	$HgDHU_2Cl_2$	DHU
N(1)–C(2)	1.31 (4)	1.335 (5)
C(2)–N(3)	1.42 (3)	1.395 (5)
N(3)–C(4)	1.35 (4)	1.364 (5)
C(4)–C(5)	1.47 (4)	1.515 (6)
C(5)–C(6)	1.52 (5)	1.507 (6)
C(6)–N(1)	1.42 (4)	1.464 (5)
C(2)–O(2)	1.23 (4)	1.222 (4)
C(4)–O(4)	1.23 (3)	1.211 (5)
Angle	**Bond Angles (deg)[b]**	
N(1)–C(2)–N(3)	114 (2)	116.1 (2)
C(2)–N(3)–C(4)	126 (2)	126.7 (2)
N(3)–C(4)–C(5)	166 (2)	115.1 (3)
C(4)–C(5)–C(6)	112 (2)	112.6 (3)
C(5)–C(6)–N(1)	108 (2)	110.3 (3)
C(6)–N(1)–C(2)	126 (2)	122.1 (2)
N(1)–C(2)–O(2)	128 (2)	124.4 (2)
N(3)–C(2)–O(2)	119 (2)	119.5 (2)
N(3)–C(4)–O(4)	121 (2)	120.9 (2)
C(5)–C(4)–O(4)	123 (2)	123.9 (3)

[a] Estimated standard deviations in parentheses are in the last digit. [b] Estimated standard deviations in degree in parentheses.

involve two short Hg–Cl bonds (2.30 and 2.28 Å), two longer Hg–Cl bonds (3.05 and 3.07 Å), and two long Hg–O bonds (2.71 and 2.88 Å). In $HgCl_2$ itself, mercury is bonded to three pairs of chlorine atoms at distances of 2.25, 3.34, and 3.63 Å, respectively. The $HgCl_2$ structure possesses three-dimensional chlorine bridging. Replacement of two chlorine atoms by pyrimidines reduces the bridging to chains in the case of uracil and sheets in the case of dihydrouracil. In the former the Hg–Cl–Hg valence angle is 93.7° while in the latter it is only 82.4°. The shortest Hg $\cdots$ Hg distances are 3.951 Å in the uracil complex and 3.564 Å in the dihydrouracil complex.

The dominant features of these structures is the $HgCl_2$-bridged arrays and the ribbons of hydrogen-bonded bases. The structure of the uracil complex can be viewed as *ribbons* of $HgCl_2$ bonded with ribbons of hydrogen bonded uracil molecules; while the dihydrouracil complex, *sheets* of $HgCl_2$ molecules bonded with ribbons of hydrogen-bonded dihydrouracil molecules.

The metallic radius of mercury is between 1.50 and 1.73 Å. Based on these values and known nonbonded contacts in various crystal structures, Grdenic (1965) has established the criterion that mercury–ligand approaches of less than 1.73 Å are considered to be valid bonds. Using the present mercury–oxygen and mercury–chlorine bond lengths and van der Waals radii of 1.4 and 1.8 Å for oxygen and chlorine, respectivey, it is clear that the observed lengths correspond to moderate to strong mercury–ligand bonds.

The structure of 1:1 $HgCl_2$–cyclohexane-1,4-dione has

TABLE VIII: Deviations of the Atoms from the Least-Squares Planes for Dihydrouracil–Mercury(II) Chloride.[a]

Atom	1	2
N(1)	**0.12**	**−0.03**
C(2)	**0.09**	**0.05**
N(3)	**−0.02**	**−0.05**
C(4)	**−0.05**	**0.03**
C(5)	**0.25**	0.20
C(6)	**−0.28**	−0.43
O(2)	0.26	0.24
O(4)	−0.30	−0.12
Hg	−0.076	−0.845
l	0.937	0.945
m	0.119	0.026
n	−0.329	−0.327
d	3.378	2.837

[a] The equations of the planes and the atoms included in calculation of the planes are defined in the same manner as in Table VI.

TABLE IX: Torsional Angles[a] for Dihydrouracil–Mercury(II) Chloride and Dihydrouracil.

Angle A–B–C–D	Dihydrouracil–Mercury(II) Chloride	Dihydrouracil[b]
C(6)–N(1)–C(2)–N(2)	11.8	13.0
N(1)–C(2)–N(3)–C(4)	12.9	11.1
C(2)–N(3)–C(4)–C(5)	−1.8	−3.0
N(3)–C(4)–C(5)–C(6)	−29.6	−26.2
C(4)–C(5)–C(6)–N(1)	47.7	45.4
C(5)–C(6)–N(1)–C(2)	−41.4	−41.0

[a] The torsional angle A–B–C–D is the projected angle between AB and CD. When viewed down the B–C bond, the clockwise rotation of bond C–D with reference to bond A–B is considered positive. [b] Rohrer and Sundaralingam (1970).

TABLE X: Bond Lengths and Bond Angles in the Mercury Coordination Sphere.[a]

Uracil Complex		Dihydrouracil Complex
Bond Lengths (Å)		
Hg–O(4)	2.71 (2)	2.88 (3)
Hg–Cl(1)	3.067 (6)	3.053 (9)
Hg–Cl(2)	2.299 (6)	2.284 (8)
Bond Angles (deg)		
O(4)–Hg–Cl(1)	84.4 (0.8)	87.6 (0.9)
O(4)–Hg–Cl(2)	90.4 (0.8)	85.9 (0.8)
Cl(1)–Hg–Cl(2)	86.3 (0.4)	89.0 (0.4)
Hg(1)–Cl–Hg(2)	93.7 (0.4)	82.4 (0.4)
Hg(1)$\cdots$Hg(2)	3.951	3.564

[a] Estimated standard deviations are in parentheses.

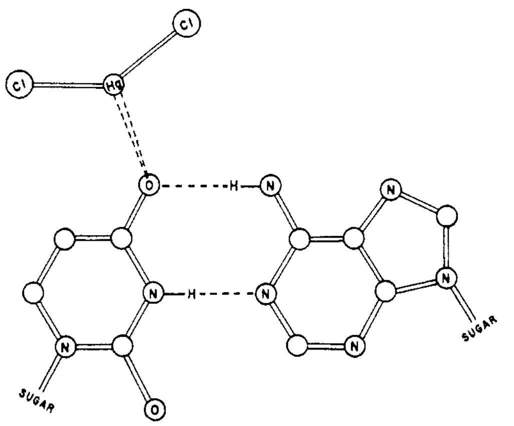

FIGURE 5: Possible mode of complex formation between AT pair of DNA and $HgCl_2$. The Hg coordination can be completed by neighboring residues of the DNA and/or solvent molecules.

been reported (Groth and Hassel, 1964) wherein both keto groups are bonded to different mercury atoms. The Hg–O distance is 2.79 Å, which compares well to the present values. The mercury atom lies in a mirror plane and is bonded to two chlorine atoms at distances of 2.30 Å. The structure is distorted octahedral, but the other bond distances are not given. The compound bis(biuret)mercury(II) chloride is reported to be isostructural with the corresponding cadmium compound (Calvalca *et al.*, 1960). The latter bears a striking resemblence to the complexes reported here. The metal is octahedrally coordinated and is chlorine bridged, as in the present case. Two metal to amide bonds complete the coordination. The structure of the mercury compound has not been reported hence bond-length comparisons cannot be made.

Mercury Binding and AT Selectivity. The present results involve mercury with bases rather than with nucleosides or nucleotides. Accordingly, they offer no unequivocal evidence for the nature of mercury interaction with DNA. However, two principle features of the structures, the binding of mercury to O(4) and combination as $HgCl_2$ rather than as Hg^{2+}, allows some reasonable inferences when compared to previous results. While the earlier work dealt primarily with mercury–thymine interactions, it is felt that the observations regarding thymine (5-methyluracil) apply generally to uracil as well. The earlier reports cite the following evidence for complex formation between Hg^{2+} ion and the nitrogen sites on the bases. (1) Mercury–nitrogen bonding is said to be generally stronger than mercury–oxygen bonding. (2) Complexation of DNA by mercury is accompanied by proton release. This implies deprotonation, *e.g.*, of N(3) of uracil or thymine, providing an available lone pair of electrons for Hg^{2+} binding. (3) Essentially the same results are achieved with $Hg(ClO_4)_2$ as with $HgCl_2$. (4) The binding is reversible with the addition of a strongly complexing anion, *e.g.*, Cl^-. (5) Insertion of Hg^{2+} between two nitrogen donors allows the linear configuration preferred by mercury in its compounds.

The present results clearly show mercury–oxygen bonding as opposed to mercury–nitrogen bonding. Not only is the criterion of Grdenic satisfied, but also the O(4) atom of uracil is significantly out of the least-squares plane of the uracil ring in the direction of mercury. The same atom in the dihydrouracil complex is also out of plane in the direction of mercury, however, in this case, the saturation of the base presents a complicating factor.

Nandi *et al.* (1965) observed the release of two protons when $HgCl_2$ was added to DNA at pH 9. Hydrolysis of $HgCl_2$ itself at this pH would release two protons. However, spectral evidence shows that mercury is bound to DNA, accordingly, $HgCl_2$ *per se*, is not available for hydrolysis. They suggest deprotonation of the nitrogen bases as the source of proton release as follows.

$$HgCl_2 + H_2B_2 \rightleftarrows HgB_2 + 2H^+ + 2Cl^- \qquad (1)$$

where H_2B_2 represents one base pair of DNA and B is a deprotonated base. In view of the present structural results, an alternative explanation seems reasonable, *viz.*

$$HgCl_2 + H_2B_2 \rightleftarrows H_2B_2HgCl_2 \qquad (2)$$

(complex formation)

$$H_2B_2HgCl_2 + 2\ HOH \rightleftarrows H_2B_2Hg[OH]_2 + 2H^+ \rightleftarrows 2Cl^- \qquad (3)$$

(hydrolysis of complex)

where eq 3 represents the hydrolysis of the mercuric chloride–DNA complex, $H_2B_2HgCl_2$, rather than $HgCl_2$. Whether eq 2 and 3 occur simultaneously or stepwise is not important. The important point is that the hydrogen ion release can be due to hydrolysis rather than to deprotonation of the ring nitrogen. At this point it is informative to consider the stepwise stability constants (Roberts, 1968) for Hg^{2+} with Cl^-.

$$Hg^{2+} + Cl^- \rightleftarrows HgCl^+,\ K = 10^{6.79} \qquad (4)$$

$$HgCl^+ + Cl^- \rightleftarrows HgCl_2,\ K = 10^{6.48} \qquad (5)$$

$$HgCl_2 + Cl^- \rightleftarrows HgCl_3^-,\ K = 10^{0.85} \qquad (6)$$

$$HgCl_3^- + Cl^- \rightleftarrows HgCl_4^{2-},\ K = 10^{1.00} \qquad (7)$$

These data indicate the very strong tendency for mercury to exist in aqueous solution in the combined form. It is not surprising then that the Hg–Cl bonds remain in tact in complexation with DNA bases. One might reasonably expect the base to have a lower affinity for mercury than does chloride ion. In fact, association constants (Simpson, 1964) reported methylmercuric and mercuric ions with the nucleosides are substantially lower than those in eq 4 and 5.

The observation that $Hg(ClO_4)_2$ behaves in a similar manner (point 3) is consistent with the hydrolysis scheme shown in eq 2 and 3, with the hydrated mercuric ion replacing the $HgCl_2$ molecules in eq 2, and the final hydrolysis product being the same as in eq 3. The reversal of the Hg–DNA complex formation through the addition of excess chloride is undoubtedly associated with the formation of complex ions such as those in eq 6 and 7. At the pH used, such complex formation would presumably be preceded by reversal of the equilibrium represented by eq 3.

Regarding point 5 above, it is noted that the usual stereochemistry of mercury is equally well satisfied when $HgCl_2$ is the reacting species. While it is true that two short linear bonds are characteristic of mercury coordination, it is also true that effective octahedral coordination is quite common in mercury compounds (Grdenic, 1965). Indeed, in both mercury complexes reported here mercury displays octahedral coordination with two short and two long Hg–Cl bonds. Hence, the involvement of $HgCl_2$ rather than Hg^{2+} is both chemically and structurally consistent.

The observation that mercury bonds preferentially to O(4) of uracil suggests an explanation for the unique complexing ability of mercury. As mentioned earlier, other ions, *e.g.*, Cu^{2+}, lower T_m, *i.e.*, allow thermal denaturation to occur at a lower temperature, while mercury complexes with DNA at room temperature, and has only a small effect on T_m. It seems reasonable that Cu^{2+} binds to N(3) of cytosine (Carrabine and Sundaralingam, 1968) and this site is undoubtedly utilized in the GC-selective denaturation of DNA. Presumably, in this case, a partial unwinding of the helix is required to expose the sites of Cu^{2+} attachment. However, in the case of complexation by mercury, such thermal activation may not be necessary. Consideration of Figure 5 suggests that $HgCl_2$ can approach the partially exposed O(4) from the outside, *i.e.*, in the large groove of the double-helical structure. Indeed, the potential bonding orbital of oxygen "points" in the proper direction. The relatively strong coordinate bond formed between mercury and oxygen would exert a strong electron-delocalizing effect on the entire uracil ring, disrupting the hydrogen bonds. This preliminary attack of mercury on the O(4) of uracil would serve the same function as does partial denaturation in the case of copper. Subsequently, other electron-donor sites *e.g.*, N(1) of adenine, or keto groups of neighboring thymine bases must be involved to complete the coordination spheres. It should be noted that the present results were obtained in the solid state and that the solution species need not possess the same coordination. However, it seems reasonable that the relatively strong Hg–Cl bonds, and the preferential Hg–O bonding should be characteristic of both the solid and solution states. The work of Nandi *et al.* (1965) clearly shows that $HgCl_2$ and AT-rich DNA react to form complexes in solution. It seems unreasonable to propose that gross changes in the nature of the complex should occur just prior to crystallization. In any case, further solution studies should be conducted to clarify these matters.

Our results provide an alternative explanation for the complexing behavior of mercury with DNA. It should be noted, however, that the structures reported here originated from solutions in the pH range of 4 to 5. While these conditions are similar to those used by Yamane and Davidson (1961) (who also observed proton release) the pH differs considerably from that used by Nandi *et al.* (1965) (pH $\sim$9). While the present results might be extended to the higher pH range, it is also that a different complex may form under those conditions. Again, further work is needed to resolve this question.

References

Bugg, C. E., Thomas, J., Sundaralingam, M., and Rao, S. T. (1971), *Biopolymers* (in press).

Calvalca, L., Nardelli, M., and Fava, G. (1960), *Acta Crystallogr., Sect. A 13*, 594.

Carrabine, J. A., and Sundaralingam, M. (1968), *Chem. Commun.*, 746.

Cromer, D. T., and Waber, J. T. (1965), *Acta Crystallogr., Sect. A 18*, 104.

Eichhorn, G. L., and Clark, P. (1963), *J. Amer. Chem. Soc. 85*, 4020.

Eichhorn, G. L., and Shin, Y. A. (1968), *J. Amer. Chem. Soc. 90*, 7323.

Grdenic, D. (1965), *Quart. Rev. (London) 19*, 303.

Groth, P., and Hassel, O. (1964), *Acta Chem. Scand. 18*, 1327.

Gruenwedel, D. W., and Davidson, N. (1966), *J. Mol. Biol. 21*, 129.

Gruenwedel, D. W., and Davidson, N. (1967), *Biopolymers 5*, 847.

Lin and Sundaralingam, M. (1971), *J. Amer. Chem. Soc.* (in press).

Matsuda, M., and Takeuchi, E. (1967), *J. Biochem. (Tokyo) 61*, 523.

Nandi, U. S., Wang, J. C., and Davidson, N. (1965), *Biochemistry 4*, 1687.

Roberts, H. L. (1968), *Advan. Inorg. Radiochem. 11*, 309.

Rohrer, D. C., and Sundaralingam, M. (1970), *Acta Crystallogr., Sect. B 26*, 586.

Simpson, R. B. (1964), *J. Amer. Chem. Soc. 86*, 2059.

Sobell, H. M., and Tomita, K. (1964), *Acta Crystallogr., Sect. A 17*, 122.

Stewart, R. F., and Jensen, L. H. (1967), *Acta Crystallogr., Sect. A 23*, 1102.

Sundaralingam, M., Rao, T., and Bugg, C. E. (1969), American Crystallography Association Meetings, Seattle, Wash.

Yamane, T., and Davidson, N. (1961), *J. Amer. Chem. Soc.*